Nature and Causes of Clear-Air Turbulence

David W. Saxton*
Air Weather Service, Scott Air Force Base, Ill.

The characteristics of clear-air turbulence (CAT) are discussed in terms of turbulence measuring systems and data reduction methods. The spectral density technique of data reduction, which has largely replaced the discrete gust method, is used to illustrate the interaction between the aircraft and turbulence and to highlight the difference between undulance and turbulence. Internal gravity waves and the conditions which appear favorable for their amplification and breakdown into isotropic turbulence are discussed. Meteorological data available to diagnose and forecast CAT are evaluated and a comparison is made between conventional rawinsonde data and wind data obtained with precision missile-tracking radar. A recent XB-70A encounter with CAT is used to illustrate the challenge of the future.

Introduction

In the early 1950's, the large number of turbojet aircraft scheduled to come into the military and civilian inventory encouraged the hope for smooth flights above the "weather." The failure to realize this hope has been largely due to sporadic and unanticipated encounters with turbulence. The term "clear-air turbulence" was used to describe these encounters because there was no visible or radar indication of convective cloud activity. The acronym, CAT, is now widely used throughout the world. It is not generally applied to all turbulence in cloud-free air, nor is it even restricted to clear air. Thus, for example, high-level turbulence in stratified cloud layers or in haze is called CAT, while low-level mechanical turbulence and turbulence in dry thermal convection are not normally termed CAT, despite the absence of clouds.

Nature of Clear-Air Turbulence

The relative frequency of significant turbulence at various altitudes is shown Fig. 1. These curves are applicable to land areas in the middle latitudes. Mechanical turbulence, a function of surface wind speed and terrain roughness, dominates the lowest few thousand feet of the atmosphere. Convective turbulence, characterized by cumuliform clouds, dominates the middle troposphere and, in periods of severe thunderstorm activity, extends as high as 60,000 ft. Clear-air turbulence dominates the upper troposphere and stratosphere, and, although it is infrequent between 50,000 and 80,000 ft, no upper limit is known. Indeed, evidence indicates that clear-air turbulence will be found at altitudes up to 100 km with a frequency maximum in the upper mesosphere.[1]

Although there is an interaction between all three types of turbulence, CAT appears to be unique in dimensions and character. This uniqueness is illustrated by the fact that CAT is normally found in thin horizontal sheets, of the order of 2000 ft thick, 10 to 20 miles in width and 50 to 100 miles in length, oriented with the wind flow pattern. Also, inflight encounters with CAT often have a rhythmic pattern, unlike the more random turbulence at lower altitudes, and repeated sharp gust loads are induced, like the bumps felt when driving an automobile over cobblestone roads. This characteristic of CAT has been recognized by the use of the term "chop" in pilot reports.

The dimensions of CAT suggest that its origin lies in the mesoscale structure of the atmosphere.[2] The rhythmic character of CAT suggest a waveform origin. It has been concluded that CAT is mainly caused by breaking gravity waves.[3] In the free atmosphere, in stable layers with wind shear, internal gravity waves with wavelengths of 3000 ft or greater can be detected. Occasionally, in the presence of moisture, their presence can be inferred by the cloud patterns generated. These long waves are not turbulent per se, at least for aircraft penetrations at subsonic speeds. They are more properly classed as undulance[1] and are characterized by laminar flow conditions.

Following Haurwitz's studies in 1931–1932 on shearing gravitational waves in billow clouds, Reiter[5] has shown that the limiting conditions between laminar and turbulent flow can be expressed by:

$$R = \Delta\rho - \frac{K\bar{\rho}}{2g}(\Delta u)^2 \begin{array}{l} < 0 \text{ unstable} \\ > 0 \text{ stable} \end{array}$$

Where $\Delta\rho$ is the density difference across the stable layer, $\bar{\rho}$ is the mean density, K is the wave number, and Δu is the wind shear.

For given conditions of density stratification and wind shear, waves shorter than a critical value will amplify exponentially and break down into isotropic turbulence. This creates an inertial subrange with wavelengths up to a few thousand feet in which energy cascades from the longer waves to the shorter waves, and the spectral density is proportional to $K^{-5/3}$, where K is the wave number of the turbulent eddies. The inertial subrange contains the scale of turbulence commonly experienced by aircraft.

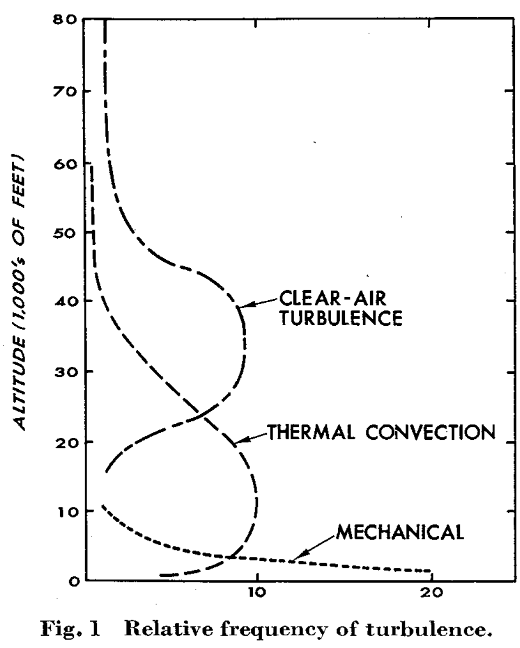

Fig. 1 Relative frequency of turbulence.

Presented as Paper 66-966 at the AIAA Third Annual Meeting and Technical Display, Boston, Mass., November 29–December 2, 1966; submitted November 17, 1966. [11.04]

* Lieutenant Colonel, U. S. Air Force; also Chief, Computer Techniques Division, Directorate of Aerospace Sciences.

It should also be noted that for given conditions of wavelength and density stratification in a layer, instability will result from increased values of vertical wind shear. In most forecasting studies, the highest consistent correlation has been found between occurrence of clear-air turbulence and strong vertical wind shear.

Turbulence Data

Most data on clear-air turbulence are derived from aircraft traverses. These data may be divided into three categories[3]: 1) those obtained subjectively from pilot reports, 2) those obtained by using the aircraft as a sensor, and 3) those obtained by using the aircraft as a platform. The vast majority of these data fall into the first category. A turbulence criteria table has been established which relates the movement of objects in the aircraft and the motion of the aircraft as a whole to the adjectival classes light, moderate, severe, and extreme. In spite of the obvious limitations inherent in this reporting system because of differences in aircraft type, airspeed, and crew experience, subjective pilot reports have formed the data base for most statistical studies on the distribution of clear-air turbulence and for the development of current forecasting methods.

The second data category is usually based upon measurements of the vertical component of acceleration at the aircraft's center of gravity. *VGH* (*V* for airspeed, *G* for vertical acceleration, *H* for altitude) recordings have been the primary method of collecting gust-loads data for many years. These data do not measure turbulence but the aircraft response to turbulence. Differences in design characteristics, weight, airspeed, and flight-level density severely restrict the wide application of data gathered by one aircraft.

To reduce this restriction, peak acceleration data collected on *VGH* records are used, in conjunction with other operating parameters, to compute derived gust velocities. The derived gust velocity concept is based on the following assumptions[4]: 1) the aircraft is a rigid body; 2) forward speed is constant; 3) the aircraft is in steady, level flight prior to penetration of a gust; 4) the aircraft can rise or fall, but cannot pitch; and 5) the vertical accelerations can be attributed to a discrete gust having a sinusoidal shape. Derived gust velocity data are usually accumulated in terms of the probability of exceeding various class limits per mile of travel. These probability values generally decrease exponentially with increasing gust velocity.[1] By 1955, the development of larger, faster, and more flexible aircraft required a more general approach to the problem of turbulence. This led to the development of power spectral techniques.

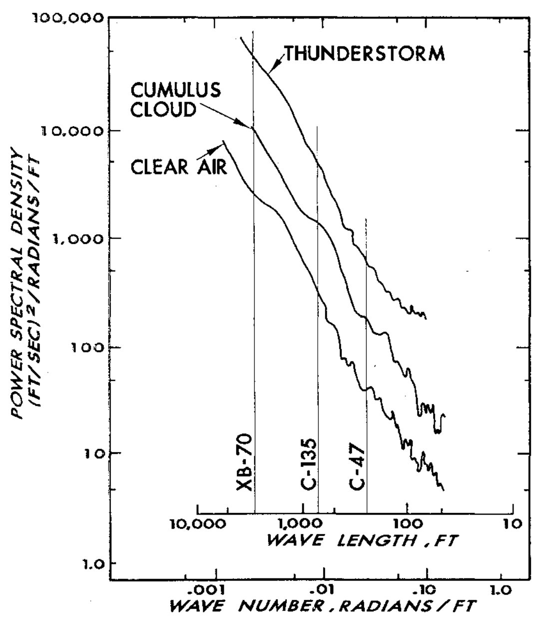

Fig. 2 Typical power spectra.

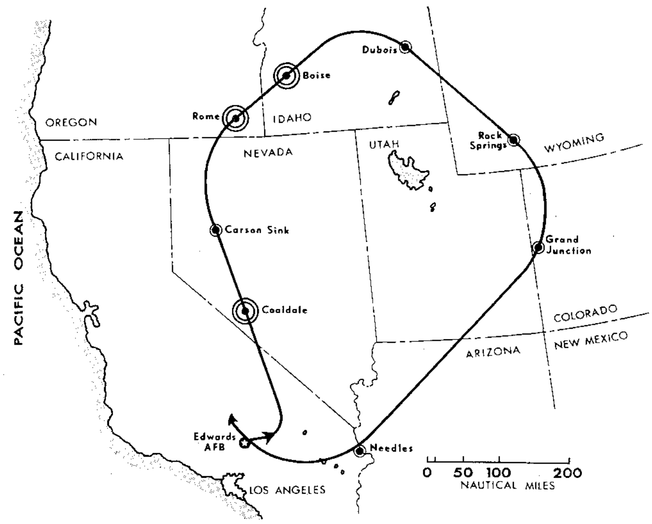

Fig. 3 XB-70 flight-test route.

The third category of data on clear-air turbulence, which uses the aircraft as a platform, provides data which are directly applicable to power spectrum analysis. The response to gust probes, either pressure-sensing elements or vanes, is interfaced through an inertial platform to remove the aircraft reactions, and true gust velocities are measured continuously.

Typical turbulence spectra (after Rhyne and Steiner[4]) are shown in Fig. 2. The ordinate can be thought of as power, with larger values representing greater levels of turbulence intensity.[4] Thus the thunderstorm spectrum shows values of turbulence intensity consistently higher than the clear-air spectrum, for all wavelengths. In general, aeronautical engineers are mainly concerned with the frequency band between 0.5 and 5 cps.[6] To illustrate the effect of airspeed on gust loads in this range of frequencies, I have plotted the wavelengths corresponding to 1 cps for three aircraft: the C-47, the C-135, and the XB-70. In this typical environment the XB-70 would encounter greater gust intensities (but not greater over all loads) in clear air at particular frequencies than a C-47 would encounter in a thunderstorm. Recent HICAT U-2 data[7] at altitudes above 50,000 feet, support this level of spectral density shown for clear air.

If clear-air turbulence results from the breakdown of gravitational shearing waves, one would expect to find a sharp spike in a spectrum corresponding to a particular wavelength. However, as pointed out by Reiter,[2] these spikes have not appeared in the limited number of spectra available to date. Instead, a few spectra show a hump that encompasses a rather broad band of wavelengths. It is hoped that future measurements, which will provide spectral data for wavelengths up to 25,000 ft, will enable researchers to define the energy levels in gravitational shearing waves and their role in creating clear-air turbulence.

The flight-test program of the XB-70, aircraft 2, which terminated so tragically in June 1966, was designed to include continuous recording of turbulence data. Unfortunately, the gust probe did not function properly, and no direct gust data are available. However, vertical, longitudinal, and lateral accelerations at the center of gravity and vertical accelerations in the cockpit were recorded.

On February 9, 1966, test flight 2–20 reported several periods of moderate turbulence during a high-speed run. Figure 3 shows the standard track flown during the flight-test program. Moderate turbulence was reported at 1058 PST, at which time the aircraft was located near Needles, Calif., at an altitude of 70,000 ft and a speed near Mach 2.9.

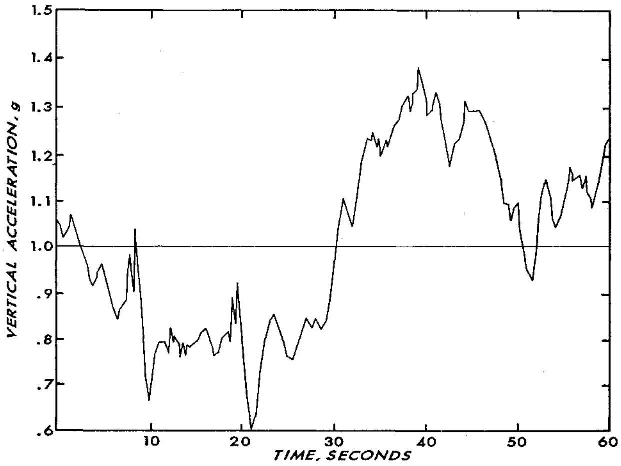

Fig. 4 XB-70 flight data, flight 2-20, February 9, 1966, 1058 PST, vertical acceleration, c.g.

In Fig. 4, the vertical-acceleration data at the center of gravity are reproduced for a 60-sec period beginning at 1058 PST. This is not an analog trace, but has been plotted from a computer output digitized at $\frac{1}{4}$-sec intervals.

The most striking feature of this record is the large-amplitude, long-period variation with a minimum near 20 sec and a maximum near 40 sec. This would correspond to a wavelength of about 20 naut miles and is not turbulence. It is impossible to determine whether this is caused by a pilot-induced maneuver or represents some large-scale undulance. The higher-frequency excursions, which are typical of turbulence, are found near 10 sec and 20 sec, for example.

Figure 5 shows the vertical accelerations in the cockpit during the same time. Although the same general large-scale character is seen, there are more fine-scale oscillations of $\frac{1}{2}$ to 2 cps. These correspond to eddy sizes of 6000 to 1500 ft, but may be due to characteristic fuselage bending modes. As these data were digitized at $\frac{1}{4}$-sec intervals, frequencies greater than 2 cps cannot be discerned. Since the cockpit is located approximately 95 ft ahead of the center of gravity, one might expect considerable enhancement of over-all loads at this point. This does not appear to be borne out in this short record. Some amplification is seen in the short period oscillation near 20 sec, but peak loads at the cockpit location remain within the envelope of peak loads at the center of gravity.

Forecasting Clear-Air Turbulence

Because of the extensive literature available on the subject of forecasting clear-air turbulence, only a brief summary will be given here. Many early studies in this field attempted to find what might be called the "magic number." That is, they sought to discover a numerical value representing a meteorological parameter or combination of parameters which was highly correlated with occurrences of clear-air turbulence and which could, when appropriately scaled, be used to forecast its occurrence and intensity.

This approach was only partly successful for three reasons. First, reports of clear-air turbulence were subjective, with wide variations in reported intensity, and only positive reports, i.e., encounters, were generally available. Secondly, the meteorological data available for operational forecasting did not provide the necessary horizontal, vertical, or temporal resolution to compute the desired parameters in the mesoscale structure where turbulence occurs. Thirdly, in those cases where significant skill was shown between occurrences of clear-air turbulence and observed meteorological parameters, it was largely lost in forecasting the desired parameters.

Among the meteorological parameters which have been investigated are vertical wind shear, horizontal wind shear, vertical wind-direction change, stability, wind speed, vorticity and vorticity advection, Richardson number, divergence, deformation, temperature gradient, thermal wind, temperature advection, and various combinations of these. For significant intensities of clear-air turbulence (moderate or greater), the highest consistent correlations have been found between encounters and vertical wind shear.[1, 8]

Wind shears of 6 knots/1000 ft (10^{-2} per sec) are generally associated with areas of moderate clear-air turbulence,[9] and 10 knots/1000 ft, with areas of severe turbulence. The problem, then, is centered on how well we measure, report, and forecast vertical wind shear.

In current rawinsonde techniques, which provide the bulk of all high-level upper wind data, winds are derived from mean values averaged over two minutes (2000 ft) to eliminate "hunting" errors in the radio direction-finding equipment. A precision missile-tracking radar system, the FPS-16, following a special superpressure balloon, the Jimsphere, has produced a limited number of very-high-quality observations of winds aloft.[10] Since some of these data are nearly concurrent with conventional rawinsonde data obtained with a GMD-1, it is possible to evaluate this latter data using the FPS-16 Radar/Jimsphere as a standard.

In Fig. 6, wind-speed profiles are shown for both types of data. The GMD-1 data were taken at Cape Kennedy on April 27, 1965. Computer output is available at this location so that wind data are derived every 1000 ft (approximately 300 m). The FPS-16 data were taken at the same location with a release time of 2314Z. Due to differences in rates of ascent, the data are only a few minutes apart at the altitudes shown. Although the FPS-16 data are tabulated

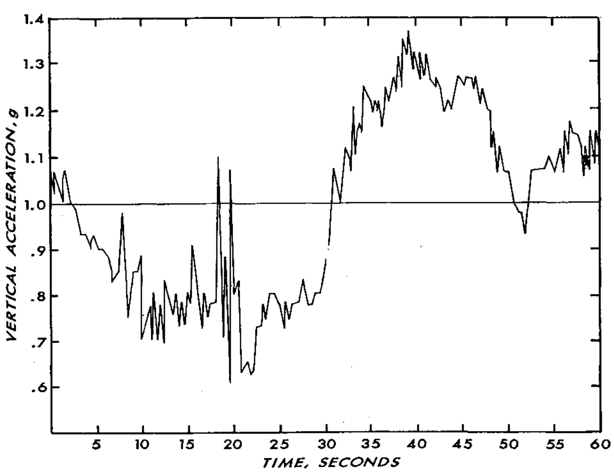

Fig. 5 XB-70 flight data, flight 2-20, February 9, 1966, 1058 PST, vertical acceleration, cockpit.

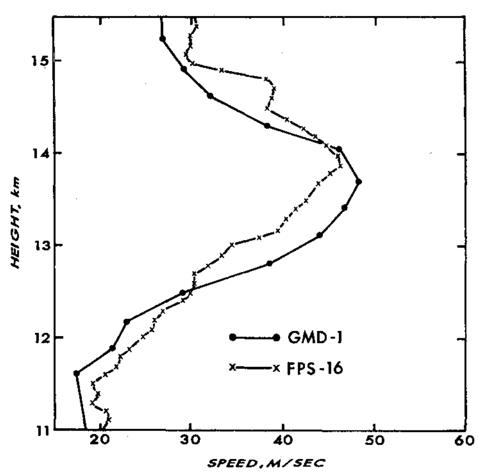

Fig. 6 Wind data, Cape Kennedy, April 27, 1965, 2323Z.

for every 25 m, only the points at 100-m intervals are plotted here, and the wind shears are computed directly for this interval without recourse to intermediate values. Both sets of data give a typical profile of a high-altitude jet stream. However, the FPS-16 data show the tendency for shear layers to be separated by "mixed" layers with little change in speed, as shown, for example, near 14.5 and 15 km.

This is illustrated in Fig. 7 where the vector wind shears have been computed. Shear values smaller than 1.5×10^{-2} are not shown in order to emphasize the significant areas. In the GMD-1 data, the maximum shear is about 3×10^{-2} sec^{-1} near 12.6 km. In the FPS-16 data, thin layers are found just below and above this layer with no significant shear between 12.4 and 12.9 km. Similarly, above 14 km, GMD-1 data depict a single thick layer, while the FPS-16 data show multiple thin layers capped by a very strong shear zone, greater than 6×10^{-2} sec^{-1}, near 15 km. No aircraft reports valid at this time were available over Florida to verify the existence of CAT at these altitudes.

As illustrated by Reiter,[5] the value of conventional rawinsonde data for computation of wind shear is further diluted by the process of encoding it for teletypewriter transmission. Mandatory reporting levels are about 5000 ft apart, significant point requirements are not a function of wind shear, and wind directions are rounded to the nearest ten degrees. In a jet stream with wind speeds near 100 knots, this latter effect alone will produce errors in wind shear which average about 10^{-2} sec^{-1} for wind reports at 1500-ft intervals.

The final stage of the problem is associated with forecasting wind shear. Unfortunately, multilevel prediction models programmed for high-speed electronic computers are characterized by data levels 5000 to 10,000 ft apart in the upper troposphere and lower stratosphere. These models are designed to forecast the large-scale flow pattern and they produce vertical wind-shear values which are of marginal usefulness for clear-air turbulence forecasting.

In spite of this rather pessimistic appraisal of the forecast problem, significant skill is shown in operational forecasting. In the Air Weather Service, forecasting clear-air turbulence has been centralized since 1962, and currently, forecasts are produced every 12 hr at Global Weather Central, Offutt Air Force Base, Neb. On an average, these forecasts cover 6% of the airspace between 10,000 and 55,000 ft over the United States. During the past winter and spring seasons more than 50% of the CAT reports of greater than moderate intensity were located in forecast boxes valid 12 and 18 hr from basic data time.

A combination of objective and subjective techniques is used to produce these forecasts. The first step is a diagnostic phase which systematically evaluates all meteorological data for a number of characteristic parameters by procedures which are programmed on an IBM 7094 computer. The mountain wave potential is included by using graphical methods with overlays which cover the important mountain ranges. All aircraft reports of CAT are plotted to show intensity, time, location, and altitude. This step is completed by outlining the geographical area, intensity, and vertical extent of potential CAT regions, verified insofar as possible by aircraft reports, for the initial data time.

The second step is the forecast phase. The initial CAT regions are generally moved in the upper-air flow pattern with identifiable synoptic-scale features (troughs, ridges, vorticity centers, isotach maxima, etc.). Changes in intensity, size, or shape of individual regions are subjective and depend on the skill and experience of the forecaster. This step is completed with a time-phased depiction of the location, vertical extent, and intensity of all regions for a 36-hr time period. The final step is a continuous MET watch program during which all aircraft reports of CAT are plotted, new surface and upper-air data are evaluated, and forecast revisions are made, if required.

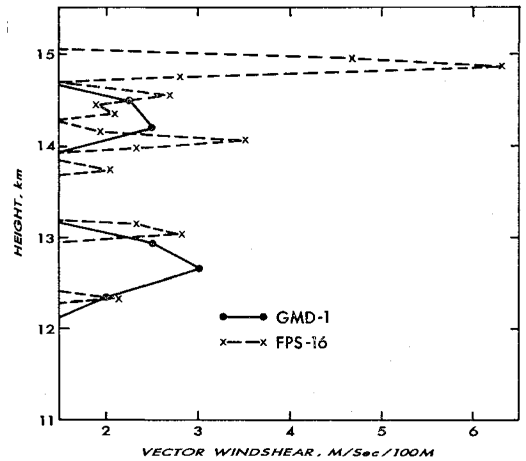

Fig. 7 Vector windshear, Cape Kennedy, April 27, 1965.

Conclusions

The rough-air problem at high altitudes can never be completely solved by forecasting. The synoptic-scale network, with an average distance between rawinsonde reports over the United States of about 300 miles and reporting intervals of 6 to 12 hr, does not provide the resolution required to forecast areas of CAT with great precision. The answer to short-period warning must be in direct detection, but this appears to be at least five years away from operational feasibility. In the meantime, better forecasting can result from two sources: 1) an objective reporting system for all in-flight encounters to provide the forecaster with a numerical measure of intensity, and 2) an improved meteorological data system to enable the forecaster to diagnose and forecast the fine-scale structure of the upper atmosphere.

We must anticipate the time, perhaps within this century, when aerodynamic lift vehicles will cruise at altitudes between 100,000 and 300,000 ft at speeds around Mach 10. Conventional clear-air turbulence characterized by wavelengths less than 1000 ft will then be felt only as noise, and large-scale turbulence and undulance with wavelengths of 1 to 10 miles will present a new challenge to designers, operators, and forecasters.

References

[1] Hildreth, W. W., Jr., et al., "High-altitude clear-air turbulence," Aeronautical Systems Div. ASD-TR-63-440 (September 1963).

[2] Reiter, E. R., "Clear air turbulence: Problems and solutions," *Proceedings of the ION-SAE Clear Air Turbulence Conference* (Society of Automotive Engineers, Inc., New York, 1966).

[3] Reiter, E. R., "The fine-scale structure of atmospheric turbulence," Colorado State Univ., Atmospheric Science Miscellaneous Rept (July 1955).

[4] Rhyne, R. H. and Steiner, R., "Turbulence and precipitation problems associated with operation of supersonic transports," Paper presented at the Fourth Conference on Applied Meteorology (1962).

[5] Reiter, E. R., *Jet Stream Meteorology* (University of Chicago Press, 1963), pp. 25–27, 207–210.

[6] Zbrozek, J. K., "Aircraft and atmospheric turbulence," *Atmospheric Turbulence and Its Relation to Aircraft* (Her Majesty's Stationery Office, London, 1963), pp. 5–42.

[7] Crooks, W., "High altitude clear air turbulence," Flight Dynamics Lab. AFFDL-TR-65-144 (September 1965).

[8] Kronebach, G. W., "An automated procedure for forecasting clear-air turbulence," J. Appl. Meteor. **3**, 119–125 (April 1964).

[9] Clarke, R. H., "Turbulence and the detailed structure of a subtropical jet stream," Univ. of Melbourne, Project TOPCAT Meteorological Reports (July 1965).

[10] Scoggins, J. R. and Susko, M., "FPS-16 radar/Jimsphere wind data measured at the eastern test range," NASA TM X-53290 (July 9, 1965).